Comparative Characterization of a Wild Type and Transmembrane Domain-Deleted Fatty Acid Amide Hydrolase: Identification of the Transmembrane Domain as a Site for Oligomerization†

Matthew P. Patricelli,‡ Hilal A. Lashuel,§ Dan K. Giang,‡ Jeffery W. Kelly,§ and Benjamin F. Cravatt*,‡

Departments of Chemistry and Cell Biology, Skaggs Institute for Chemical Biology, The Scripps Research Institute, 10550 North Torrey Pines Road, La Jolla, California 92037

Received July 17, 1998; Revised Manuscript Received August 25, 1998

ABSTRACT: Fatty acid amide hydrolase (FAAH) is an integral membrane protein responsible for the hydrolysis of a number of primary and secondary fatty acid amides, including the neuromodulatory compounds anandamide and oleamide. Analysis of FAAH's primary sequence reveals the presence of a single predicted transmembrane domain at the extreme N-terminus of the enzyme. A mutant form of the rat FAAH protein lacking this N-terminal transmembrane domain (ΔTM-FAAH) was generated and, like wild type FAAH (WT-FAAH), was found to be tightly associated with membranes when expressed in COS-7 cells. Recombinant forms of WT- and ΔTM-FAAH expressed and purified from *Escherichia coli* exhibited essentially identical enzymatic properties which were also similar to those of the native enzyme from rat liver. Analysis of the oligomerization states of WT- and ΔTM-FAAH by chemical cross-linking, sedimentation velocity analytical ultracentrifugation, and size exclusion chromatography indicated that both enzymes were oligomeric when membrane-bound and after solubilization. However, WT-FAAH consistently behaved as a larger oligomer than ΔTM-FAAH. Additionally, SDS−PAGE analysis of the recombinant proteins identified the presence of SDS-resistant oligomers for WT-FAAH, but not for ΔTM-FAAH. Self-association through FAAH's transmembrane domain was further demonstrated by a FAAH transmembrane domain−GST fusion protein which formed SDS-resistant dimers and large oligomeric assemblies in solution.

Fatty acid amide hydrolase (FAAH)[1] (*1*−*5*) is the only identified mammalian member of a family of amidase enzymes known as the "amidase signature" family (*6*). Despite the presence of these enzymes in prokaryotic (*6*−*10*) and eukaryotic (*1*, *11*−*13*) organisms, little is yet known about their catalytic mechanism and structural features.

Among the amidase signature enzymes, FAAH is of particular interest due to the intriguing biological activities of its fatty acid amide substrates. Several fatty acid amides, including the neuromodulatory compounds anandamide and oleamide, have recently been identified as important mammalian signaling molecules (*14*−*18*). Anandamide (arachidonoyl ethanolamide) was first characterized as an endogenous brain ligand for the CB1 cannabinoid receptor (*15*) and has since been shown to possess cannabinoid-like properties in vivo (*19*). Oleamide (9-*Z*-octadecenamide) was isolated from the cerebrospinal fluid of sleep-deprived cats (*20*), found to induce physiological sleep when injected into rats (*14*), and shown to modulate 5-hydroxytryptamine (5-HT) receptor responses to serotonin (*21*−*23*). FAAH is highly expressed in neurons within the central nervous system where the enzyme appears poised to inactivate fatty acid amides at their presumed sites of action (*24*, *25*). Consistent with this notion, addition of FAAH inhibitors to neuroblastoma cell cultures increased the amounts of anandamide (*26*) and oleamide (*27*) produced by these cells, and FAAH-resistant analogues of anandamide have been shown to induce prolonged inhibition of motor activity in rats (*28*).

Due to the hydrophobic nature of FAAH's substrates, intimate interactions between the enzyme and cell membranes may be important for efficient rates of substrate hydrolysis and product release. It is thus not surprising that unlike most other amidase signature enzymes, FAAH is an integral membrane protein, a feature which has in turn rendered the structural and enzymological characterization of FAAH particularly challenging. Defining the nature of FAAH's membrane interactions, as well as the role that these associations play in the enzyme's structure and function, may prove essential to a deeper understanding of how FAAH participates in the regulation of fatty acid amide signaling in vivo.

Primary sequence analysis of the mouse, rat, and human FAAH proteins predicts that these enzymes are type I integral

† This work was supported by grants from the NIH (MH58542 to B.F.C. and GM51105 to J.W.K.), the Skaggs Institute for Chemical Biology (B.F.C. and J.W.K.), the Searle Scholars Program (B.F.C.), the National Science Foundation (predoctoral fellowship for M.P.P.), and the American Chemical Society (predoctoral fellowship for H.A.L.).

* To whom correspondence should be addressed. Telephone: (619) 784-8633. Fax: (619) 784-2345. E-mail: cravatt@scripps.edu.

‡ Department of Cell Biology.

§ Department of Chemistry.

[1] Abbreviations: FAAH, fatty acid amide hydrolase; WT-FAAH, wild type rat FAAH; ΔTM-FAAH, transmembrane domain-deleted rat FAAH; PCR, polymerase chain reaction; GST, glutathione *S*-transferase; CHAPS, 3-[(3-cholamidopropyl)dimethylammonio]-1-propanesulfonate; SDS−PAGE, sodium dodecyl sulfate−polyacrylamide gel electrophoresis; BMH, bismaleimidohexane; DTT, dithiothreitol; EDTA, ethylenediaminetetraacetic acid; C_8E_5, *n*-octyl pentaoxyethylene; LDAO, lauryl dimethylamineoxide; His, histidine; 5-HT, 5-hydroxytryptamine; R_s, Stokes radius.

10.1021/bi981733n CCC: $15.00
Published on Web 10/08/1998

membrane proteins with a single transmembrane domain from amino acids 9 to 29 and a large cytoplasmic tail containing the majority of the protein sequence (amino acids 30−579; TMpred and PSORT prediction programs). To elucidate the role of the transmembrane domain in FAAH's membrane binding, catalytic, and self-association properties, we have characterized an N-terminal transmembrane domain deletion construct of rat FAAH (ΔTM-FAAH) and compared this mutant enzyme to the wild type protein (WT-FAAH).

EXPERIMENTAL PROCEDURES

Generation of FAAH Expression Constructs. The locations of potential transmembrane domains in human, mouse, and rat FAAH were predicted using PSORT (http://psort-.nibb.ac.jp:8800/form.html) and TMpred (http://www.isrec.isb-sib.ch/software/TMPRED_form.html) analysis programs. The ΔTM-FAAH construct for subcloning into the eukaryotic expression vector pcDNA3 (Invitrogen) was generated by PCR from the cloned rat WT-FAAH cDNA using the following primers: sense primer, 5′-GCGGTACCATGCGATGGACCGGGCGC-3′; and antisense primer, 5′-GGTCTGGCCAAAGAGAGG-3′. The sense primer contained an added *Kpn*I site and in-frame ATG for creating an artificial translation initiation site. An approximately 520 bp PCR product was generated, digested with *Kpn*I−*Hin*dIII, and subcloned into a *Kpn*I−*Hin*dIII-digested WT-FAAH pcDNA3 vector to generate the ΔTM-FAAH-pcDNA3 construct (amino acids 30−579). The WT-FAAH pcDNA3 construct has been described previously (*1*). The calculated molecular masses of the COS-7-expressed WT- and ΔTM-FAAH are 63.3 and 60.1 kDa, respectively. The ΔTM-FAAH construct for subcloning into the prokaryotic expression vector pTrcHisA (Invitrogen) was generated by PCR from the cloned rat FAAH cDNA using the following primers: sense primer, 5′-GCCTCGAGACCGGGCGCCAGAAGG-3′; and antisense primer, 5′-GCGAATTCTCACGATGGCTGCTTTTGAGG-3′. The resulting PCR product was ligated into the pTrcHisA vector to generate an N-terminally His-tagged ΔTM-FAAH construct (amino acids 32−579). A WT-FAAH cDNA was generated by PCR using the following primers: sense primer, 5′-GCCTCGAGGATGGTGCTGAGCGAAG-3′; and antisense primer, 5′-GCGAATTCCGATGGCTGCTTTTGAGG-3′. This cDNA was ligated into the pTrcHis2C vector to generate a C-terminally His-tagged WT-FAAH construct. The calculated molecular masses of the *Escherichia coli*-expressed WT- and ΔTM-FAAH are 67.2 and 64.5 kDa, respectively. A C-terminally His-tagged ΔTM-FAAH and N-terminally His-tagged WT-FAAH were similarly generated. All constructs were confirmed by sequencing in both directions.

Generation of a FAAH Transmembrane Domain−GST Fusion Protein. A GST construct for subcloning into the WT-FAAH-pTrcHis2 vector was generated by PCR from the expression vector pGEX4T-3 (Amersham Pharmacia Biotech) using the following primers: sense primer, 5′-CGCCCGGGGCATGTCCCCTATACTAGG-3′; and antisense primer, 5′-CGGAATTCTAGATTAAACCAGATCCGATTTTGG-3′. A cDNA containing the coding sequence of GST with a 5′-*Sma*I site, 3′-*Eco*RI site, and 3′ stop codon was thereby generated and ligated into the WT-FAAH pTrcHis2C construct using an internal *Sma*I site of the rat FAAH cDNA and a vector *Eco*RI site. The resulting construct encoded a fusion protein containing residues 1−39 of FAAH and the entire GST sequence, terminating in a stop codon so incorporation of the C-terminal His tag could be prevented. The GST fusion vector pGEX4T-3 was used to express wild type GST. The calculated molecular masses of the expressed GST and TM−GST proteins are 27.8 and 30.0 kDa, respectively.

Generation of Anti-FAAH and Anti-GST Polyclonal Antibodies. Rabbit polyclonal antibodies were raised against a FAAH−GST fusion protein (including amino acids 38−579 of the rat FAAH protein) generated by standard molecular biology procedures (Amersham Pharmacia Biotech). Affinity purification of the anti-FAAH rabbit antibodies was conducted by first depleting rabbit antiserum of GST-cross reactive antibodies (which constituted affinity-purified anti-GST antibodies) and then isolating from this serum the FAAH−GST reactive antibodies.

COS-7 Expression and Analysis. Transient transfections, immunofluorescence, and fractionation of COS-7 extracts into cytosolic and membrane fractions were performed as previously detailed, with an additional step where total cell extracts were sonicated following Dounce homogenization (*12*). Where indicated, membrane pellets were resuspended in 200 μL of 100 mM Na_2CO_3 by sonication. The resuspended pellet was incubated in 100 mM Na_2CO_3 for 30 min at 4 °C and then airfuged at 30 psi for 30 min. The 100 mM Na_2CO_3 supernatant was airfuged once more at 30 psi for 30 min, while the 100 mM Na_2CO_3 pellet was resuspended in 200 μL of 100 mM Na_2CO_3. An analogous protocol was employed for treating cell membranes under high-salt conditions [1.0 M NaCl in a buffer of 12.5 mM Hepes (pH 8.0) and 1 mM EDTA]. Protein concentrations of each fraction were determined (D_c protein assay kit, Bio-Rad), and 10 μg of protein from each fraction was analyzed by standard SDS−PAGE and Western blotting procedures. All SDS−PAGE protein samples, both here and in subsequently discussed studies (unless otherwise indicated), were incubated in 2× loading buffer [125 mM Tris (pH 6.75), 20% glycerol, 4% SDS, 10% β-mercaptoethanol, and 0.005% bromophenol blue] and heated for 5 min at 90 °C prior to SDS−PAGE analysis. For analysis of FAAH activity in intact COS-7 cells, [^{14}C]oleamide [1 μCi, 50 μCi/μmol, synthesized as described previously (*14*)] in ethanol (4 μL) was added to 5 mL of complete medium (DMEM with L-glutamine, nonessential amino acids, sodium pyruvate, and 10% fetal bovine serum), and the resulting solution was applied to a 100 mM dish of transiently transfected COS-7 cells (on the second day of transfection, 80−90% confluency). Following a 15 min incubation at 37 °C, the medium was removed, and the cells were washed with 2 × 5 mL volumes of complete medium and then harvested by cell scraping. The resulting cell suspension was extracted with ethyl acetate (3 volumes), and the organic layer was removed and concentrated under a stream of nitrogen. The dried organic extract was resuspended in 20 μL of ethanol and analyzed by thin layer chromatography (TLC; solvent conditions of 55% ethyl acetate/hexanes; oleamide with an R_f of 0.4), and radiolabeled lipids were quantified by phosphorimaging (Packard). Relative oleamide concentrations were calculated as percent values of the total radioactivity on the TLC plates.

Purification of WT- and ΔTM-FAAH from E. coli. The WT- and ΔTM-FAAH proteins were expressed in the *E. coli* BL21(DE3) strain by following manufacturer's guidelines (Invitrogen). Cultures were induced with 1 mM IPTG at an OD_{600} of 0.6−0.7. The cultures were induced for 4 h and pelleted at 5000*g* for 20 min. At this point, the cell pellets could be frozen at −80 °C. The cells were resuspended in 80 mL of lysis buffer [50 mM Tris (pH 8.0), 100 mM NaCl, and 1% Triton X-100], and lysozyme was added to a final concentration of 1 mg/mL. Triton X-100 in the lysis buffer was found to be necessary for recovery of both WT- and ΔTM-FAAH. After incubation on ice for 30 min, the lysate was sonicated with a 50 W tip sonicator with six to ten 10 s pulses and centrifuged at 10000*g* for 35 min. The resulting supernatant was added to a 2 mL bed volume of Talon cobalt affinity resin (Clontech) and the mixture placed on a rotating wheel for 30 min at room temperature. The beads were collected by centrifugation at 700*g* for 5 min and washed in batch with 30 mL of lysis buffer and twice with 30 mL of lysis buffer and 10 mM imidazole before applying to a 1.5 × 30 cm column. The column was washed once with 15 mL of lysis buffer and 10 mM imidazole, and the bound protein eluted with 6 mL of elution buffer (lysis buffer and 200 mM imidazole). The eluted protein was next applied to a 4 mL bed volume of heparin−agarose (Bio-Rad) pre-equilibrated in the imidazole elution buffer. Heparin purification was carried out immediately following elution from the Talon resin as the enzymatic activity was unstable to freezing or prolonged storage at 4 °C in the imidazole elution buffer. The column was rinsed sequentially with 15 mL of imidazole elution buffer, 20 mL of buffer 1 [20 mM Hepes (pH 7.8), 10% glycerol, 1 mM EDTA, and 0.5% CHAPS] with 150 mM NaCl, and 20 mL of buffer 1 with 300 mM NaCl. The purified ΔTM-FAAH was eluted with 6 mL of buffer 1 with 700 mM NaCl, and WT-FAAH was eluted with 6 mL of buffer 1 with 1.0 M NaCl. Following purification, the proteins were concentrated and desalted using a Millipore UltraFree-15 centrifugal filter device (30 K NMWL).

Sucrose gradient purification was performed by adding 500 μg of WT- or ΔTM-FAAH to a 12.5 mL gradient of 5 to 20% sucrose in buffer 2 [20 mM Hepes (pH 7.8), 0.5% CHAPS, 1 mM EDTA, 150 mM NaCl, and 1 mM DTT]. The gradients were centrifuged at 39 000 (ΔTM-FAAH) or 32 000 rpm (WT-FAAH) for 14 h in a Beckman LE-80K ultracentrifuge using an SW-40 rotor. Gradients were drained in 1 mL fractions, and fractions containing FAAH were identified by SDS−PAGE. Sucrose was removed using centrifugal filtration devices as described above. The concentration of purified FAAH was determined with the Bio-Rad D_c protein assay kit, and this value was correlated with the UV absorbance of the protein at 280 nm. A solution with an A_{280} of 0.8 was found to contain approximately 1 mg/mL recombinant FAAH. This value was used for all subsequent concentration measurements.

Expression and Purification of GST and TM−GST. Both proteins were expressed and purified from the *E. coli* BL21 strain according to the manufacturer's recommendations (Amersham Pharmacia Biotech) with the following modifications. The proteins were solubilized and bound to glutathione−Sepharose in phosphate-buffered saline (PBS) with 1% Triton X-100. Following binding, this buffer was exchanged for PBS with 0.5% CHAPS. After elution, the proteins were concentrated by centrifugal filtration and further purified by gel filtration as described below.

Gel Filtration Chromatography. An AKTA purifier (Amersham Pharmacia Biotech) was used for all runs. The desired protein sample was loaded onto a Superdex 200 or Superose 6 gel filtration column (Amersham Pharmacia Biotech) equilibrated in buffer 2 at a flow rate of 0.5 mL/min, and the eluted protein was monitored by UV absorbance at 280 nm. Collected fractions were assayed for enzyme activity (FAAH samples only) and analyzed by SDS−PAGE followed by Coomassie staining and Western blotting to confirm the identity and purity of the protein contributing to the observed UV peaks. Molecular mass calibration of the Superdex 200 column was accomplished using blue dextran (to determine V_o), thyroglobin (669 kDa, R_s = 8.6 nm), ferritin (440 kDa, R_s = 6.3 nm), catalase (232 kDa, R_s = 5.2 nm), and bovine serum albumin (66 kDa, R_s = 3.5 nm), where the R_s values are predicted Stokes radii based on previous studies (*29*). The Superose 6 column was calibrated with the same markers except aldolase (158 kDa, R_s = 4.6 nm) was used in place of bovine serum albumin. The elution volumes of the markers were converted to σ values using the equation $\sigma = (V_e - V_o)/(V_T - V_o)$, where V_e is the elution volume, V_o is the column void volume, and V_T is the total column volume (determined by salt peak elution). The σ values obtained were plotted as a linear function of log(molecular weight).

Liver Plasma Membrane Preparation. Rat liver plasma membranes were isolated from 15 rat livers as described previously (*30*), combined, resuspended in 80 mL of buffer 1 with 1% Triton X-100 in place of CHAPS, and Dounce homogenized. The membrane solution was stirred at 4 °C for 2 h and then spun at 27 000 rpm for 1 h (SW-28 rotor, Beckman). The resulting supernatant constituted solubilized liver plasma membranes.

Enzyme Assays. All reactions were conducted in glass vials in a total volume of 200 μL. [^{14}C]Oleamide (25−50 μCi/mM) was dissolved in ethanol to 25 times the desired final concentration, and 4 μL was added to a glass vial with a glass syringe. Ethanol (5 μL) was added, followed immediately by 91 μL of reaction buffer [125 mM Tris and 1 mM EDTA (pH 9.0) for K_m determinations and COS-7 activity measurements or 50 mM bis-Tris, 50 mM CAPS, and 50 mM sodium citrate (pH 5−11) for pH profile measurements]. A solution of 10 μL of 4−4.5 μg/mL purified WT- or ΔTM-FAAH in buffer 1 with 1% Triton X-100 (a concentrated stock of the purified enzyme was diluted into this buffer to obtain the desired concentration) or 8 μL of the liver plasma membrane preparation was prepared in 90−92 μL of reaction buffer and the mixture added to the solution of [^{14}C]oleamide. For K_m determinations, 50 μL of the reaction mixture was removed at three time points with a glass syringe and the reaction quenched in 300 μL of 0.07 N HCl. For pH−rate profile measurements and relative rates in COS-7 transfection, the entire reaction was quenched with 600 μL of 0.07 N HCl. The reaction products were isolated and analyzed as described previously (*1*, *12*), with the exception being that quantification was conducted by phosphorimager analysis (Packard). K_m values were determined from Lineweaver−Burk plots of four substrate concentrations performed in quadruplicate. Errors

reflect the sample standard deviations of the four measurements.

Cross-Linking Studies. To normalize the levels of COS-7 expression between WT- and ΔTM-FAAH for cross-linking, transfections were performed using 1.5 μg of WT-FAAH cDNA and 5 μg of ΔTM-FAAH cDNA. COS-7 cell extracts were prepared for cross-linking by isolating membranes and diluting to approximately 4 mg/mL total protein in 12.5 mM Hepes (pH 8.0), 1 mM EDTA, and 100 mM NaCl. Five microliters of bismaleimidohexane (BMH, Pierce) was added as a 10× stock in DMSO to 50 μL of the dilute protein solution. The reaction was allowed to proceed at room temperature for 60 min before quenching with 55 μL of 2× SDS−PAGE loading buffer. The samples were heated to 90 °C for 10 min, and then 15 μL was analyzed by SDS−PAGE (4 to 12% Tris-glycine gel, Novex) and Western blotting.

Analytical Ultracentrifugation. The sedimentation properties of WT- and ΔTM-FAAH were obtained from data collected on a temperature-controlled Beckman XL-I analytical ultracentrifuge equipped with an An60Ti rotor and photoelectric scanner. A double sector cell equipped with a 12 mm Epon centerpiece and quartz windows was loaded with 400−420 μL of sample using a blunt-end microsyringe. Data were collected at rotor speeds of 3000−40000 rpm in the continuous mode at 20 °C, with a step size of 0.005 cm and an average of four scans per point. Fewer scans per point were used when fast sedimenting species were followed to allow more data sets per unit time to be collected.

Analysis of the Sedimentation Velocity Profiles. The second moment boundary sedimentation analysis was initially applied to determine the average sedimentation coefficient, *s* (reported in Svedberg units, S, where S represents 10^{-13} s), for all the species in solution. However, for rigorous analysis of solutions containing multiple species, the van Holde−Weischet global boundary analysis was used for fitting the absorbance data (*31*). The van Holde−Weischet global fitting method is especially useful for examining sample homogeneity and/or heterogeneity and facilitates a rigorous analysis of complex boundaries of multicomponent systems, yielding accurate $s_{20,w}$ values for all components present (*32*). The contribution of diffusion to the boundary shape is removed in the van Holde−Weischet analysis by extrapolating to infinite time ($t^{-1/2} = 0$), thus achieving resolution between species with similar *s* values. In the van Holde−Weischet extrapolation plots, a homogeneous sample would yield a single *y*-intercept corresponding to the diffusion-corrected sedimentation coefficient of the species in solution, while a sample that is heterogeneous would give multiple *y*-intercepts. The van Holde−Weischet analysis is not perturbed by experimentally noisy data, as Demeler and co-workers have shown that this method faithfully interprets the experimental data even at noise levels higher than those that are usually experienced with the XL-I (using simulated data) (*33*). The d*c*/d*t* time derivative analysis methods for calculating the apparent sedimentation coefficient distribution *g*(**S*) developed by Stafford was also used to evaluate and confirm the homogeneity and/or heterogeneity of the samples (*34*, *35*).

The observed sedimentation coefficient, *s*, was corrected to reflect standard conditions (water at 20 °C) with the following equation:

$$s_{20,w} = s\frac{(\eta)_{T,b}}{(\eta)_{20,w}}\frac{(1-\bar{v}\rho)_{20,w}}{(1-\bar{v}\rho)_{T,b}} \quad (1)$$

where ρ and η are the density and viscosity, respectively, of water at 20 °C and $\bar{v}$ is the partial specific volume of the protein. The density and viscosity were calculated using polynomial equations and tables of coefficients (*36*). The partial specific volume of WT- and ΔTM-FAAH (0.738 cm^3/g) was estimated on the basis of the partial specific volumes of the component amino acid residues (*37*−*39*).

RESULTS

Expression and Analysis of WT- and ΔTM-FAAH in COS-7 Cells. PCR was used to generate a rat FAAH cDNA lacking the coding region for the N-terminal transmembrane domain (ΔTM-FAAH, amino acids 30−579), and this cDNA was subcloned into the pcDNA3 eukaryotic expression vector. Homogenates from COS-7 cells transiently transfected with either the ΔTM-FAAH or wild type rat FAAH (WT-FAAH) cDNA expressed greater than 100-fold more oleamide hydrolase activity than mock-transfected COS-7 cells (transfected with an empty pcDNA3 vector). Further biochemical fractionation of the COS-7 cell extracts was conducted to determine whether the ΔTM-FAAH protein was associated with membranes. Enzymatic assays on fractionated cell extracts demonstrated that greater than 90% of the FAAH activity was found to be associated with membrane fractions for both WT-FAAH (soluble fraction, 6 nmol min^{-1} mg^{-1}; membrane fraction, 239 nmol min^{-1} mg^{-1}) and ΔTM-FAAH (soluble fraction, 7 nmol min^{-1} mg^{-1}; membrane fraction, 123 nmol min^{-1} mg^{-1}). Likewise, Western blotting using affinity-purified anti-FAAH polyclonal antibodies identified both WT- and ΔTM-FAAH in these same membrane fractions (Figure 1A, upper panel). When we incubated these membrane fractions with 100 mM Na_2CO_3 (pH 11.0), we failed to solubilize significant amounts of either WT- or ΔTM-FAAH as judged by Western blotting (Figure 1A, lower panel). This treatment resulted in the loss of oleamide hydrolase activity in these fractions. High-salt washes (1.0 M NaCl) also failed to remove either WT- or ΔTM-FAAH from COS membranes as judged by both Western blotting and enzyme activity assays (data not shown). Finally, the results from Western blotting indicated that the lower overall enzyme activity found in the ΔTM-FAAH fractions relative to the WT-FAAH fractions could be ascribed to a lower expression level of the ΔTM-FAAH protein, rather than being the result of a reduced inherent activity for the mutant enzyme. In subsequent experiments, transfection of COS-7 cells with an appropriately reduced amount of the WT-FAAH construct allowed for equivalent expression levels of WT- and ΔTM-FAAH as judged by both Western blotting and enzyme activity assays.

Immunofluorescence studies with COS-7 cells transiently transfected with either the WT- or ΔTM-FAAH construct revealed a relatively diffuse staining pattern with the highest intensity in regions near, but not including, the nucleus (Figure 1B). This staining is most compatible with predominate association of both proteins with the endoplasmic reticulum and/or Golgi apparatus. Overall, the patterns of staining observed for WT- and ΔTM-FAAH were indistinguishable at the level of resolution afforded by conventional

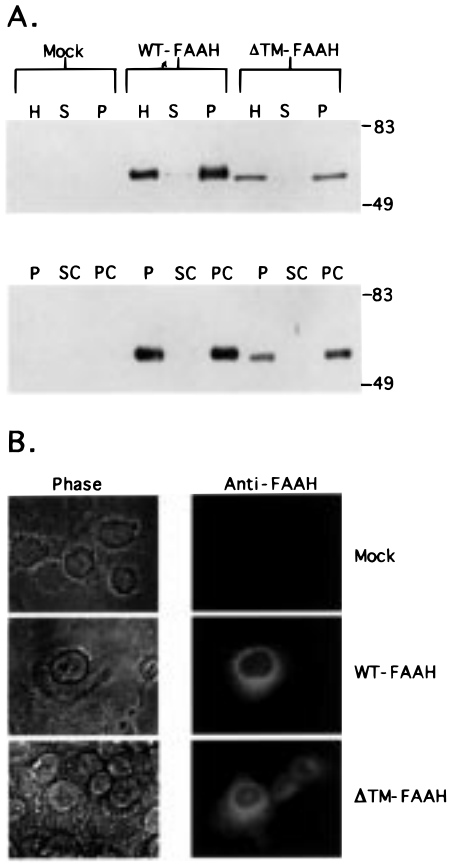

FIGURE 1: Expression and comparison of WT- and ΔTM-FAAH in COS-7 cells. (A) Western blot analysis of COS-7 cell extracts from mock-, WT-, and ΔTM-FAAH-transfected COS-7 cells identifying significant expression of both FAAH constructs in crude homogenates. Both WT- and ΔTM-FAAH immunoreactivity associated with membrane fractions upon cellular fractionation (upper panel). Following a 30 min wash with 100 mM Na_2CO_3, both WT- and ΔTM-FAAH were retained in membrane fractions (H, homogenates; S, soluble protein fraction; P, membrane fraction; SC, soluble fraction following Na_2CO_3 wash; PC, membrane fraction following Na_2CO_3 wash). Molecular mass standards are indicated in kilodaltons. (B) Immunofluorescence microscopy of transfected COS-7 cells with anti-FAAH antibodies. A similar pattern of diffuse membranous staining was observed for both WT- and ΔTM-FAAH.

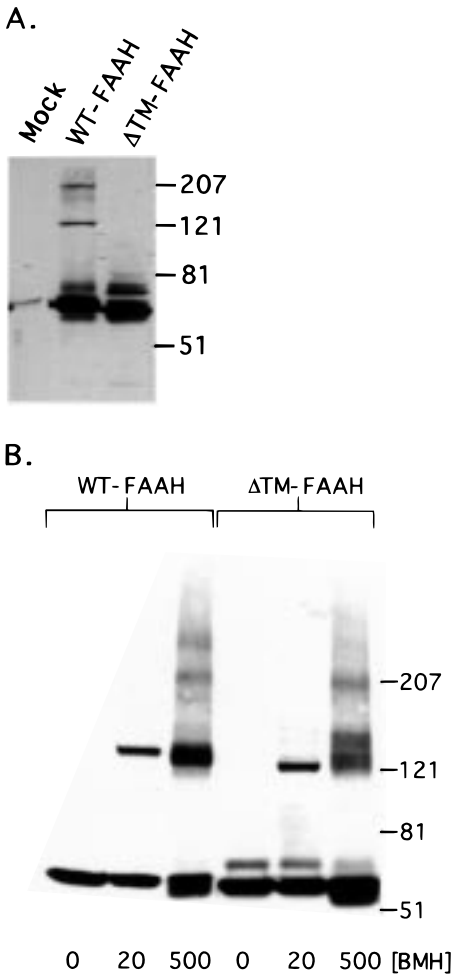

FIGURE 2: Evidence for FAAH oligomerization in transfected COS-7 cell extracts. (A) Western blot analysis of WT- (center lane) and ΔTM-FAAH (right lane) present in isolated COS-7 membranes. Samples were loaded under reducing, denaturing conditions (5% β-mercaptoethanol and 2% SDS) on a 10% polyacrylamide gel. Note the presence of potential oligomeric immunoreactive bands at ≥120 kDa for WT-FAAH which are not present in the ΔTM-FAAH sample. (B) Western blot analysis of WT- and ΔTM-FAAH from COS-7 membranes following a 1 h incubation with bismaleimidohexane (BMH) at the indicated concentrations (in micromolar). Proteins were loaded on a 4 to 12% polyacrylamide gradient gel. Molecular mass standards are indicated in kilodaltons.

fluorescence microscopy, suggesting that the two enzymes were similarly localized in COS-7 cells. Consistent with this notion, intact WT- and ΔTM-FAAH-transfected cells both showed efficient and equivalent abilities to hydrolyze oleamide added to their incubation media. When transfected COS-7 cells were incubated in media containing 1 μCi of [^{14}C]oleamide for 15 min and then harvested and their lipid contents analyzed by thin layer chromatography (TLC), the following relative oleamide levels were identified (given as a percentage of the total lipid radioactivity): mock-transfected, 47% oleamide; ΔTM-FAAH-transfected, 5% oleamide; and WT-FAAH-transfected, 7% oleamide.

Despite the overall similarity observed between WT- and ΔTM-FAAH when they are expressed in COS-7 cells, SDS−PAGE Western blotting experiments did reveal one intriguing difference between the two proteins. WT-FAAH cell extracts consistently contained low but significant levels of additional immunoreactive bands at sizes corresponding to dimeric and higher-molecular mass (possibly trimeric and/or tetrameric) forms of the enzyme, while ΔTM-FAAH cell extracts did not show these species (Figure 2A). The levels of these SDS-resistant oligomeric forms of WT-FAAH were insensitive to boiling and unaffected by the presence and/or absence of reducing agents.

Further characterization of this apparent oligomerization of FAAH was conducted by chemical cross-linking using bismaleimidohexane (BMH) (Figure 2B). Immunoreactive bands corresponding to the expected molecular masses of dimeric species were observed for both WT- and ΔTM-FAAH after incubations of transfected COS-7 membranes with 20 μM BMH for 1 h. At higher BMH concentrations (500 μM), immunoreactive bands consistent with dimeric, trimeric, and tetrameric species of WT-FAAH and ΔTM-FAAH were observed, with the relative proportion of the tetrameric species being significantly greater for WT-FAAH than for ΔTM-FAAH.

Expression and Purification of ΔTM- and WT-FAAH from E. coli. To further compare the catalytic and structural properties of WT- and ΔTM-FAAH, recombinant forms of each protein were expressed and purified from *E. coli*.

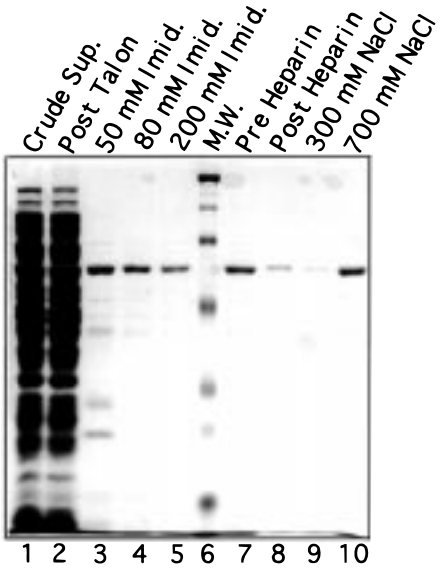

FIGURE 3: Expression and purification of ΔTM-FAAH from *E. coli*. Triton X-100-solubilized *E. coli* extracts (lane 1) containing N-terminal His-tagged ΔTM-FAAH prior to (lane 1) and after (lane 2) incubation with cobalt affinity resin. Bound FAAH was eluted with 50 (lane 3), 80 (lane 4), and 200 mM (lane 5) imidazole. Elution with a single volume of 200 mM imidazole provided similar results. The elutions were combined (lane 7) and applied to a heparin−agarose column. Heparin flow through (lane 8) indicated efficient binding of ΔTM-FAAH. The column was washed with 300 mM NaCl (lane 9) and purified ΔTM-FAAH eluted with 700 mM NaCl (lane 10). Molecular mass standards (lane 6) are from top to bottom: 207, 121, 81, 51, 34, and 29 kDa.

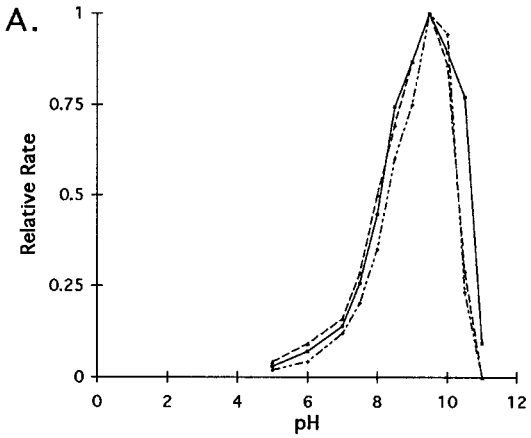

B.

	K_m (μM)	k_{cat} (s^{-1})	k_{cat}/K_m
WT-FAAH	23 ± 8	7.1	3.1×10^5
ΔTM-FAAH	12 ± 2	3.3	2.8×10^5
Rat Liver FAAH	31 ± 3	ND	ND

FIGURE 4: Enzymatic characterization of recombinant purified WT- and ΔTM-FAAH. (A) The pH−rate profiles of solubilized rat liver FAAH (solid line), WT-FAAH (dashed line), and ΔTM-FAAH (stipled line). (B) Relevant kinetic parameters obtained for recombinant WT-FAAH, ΔTM-FAAH, and native rat liver FAAH. ND, not determined.

Expression of ΔTM-FAAH in *E. coli* was accomplished by using the pTrcHisA vector to generate an N-terminal His_6-tagged fusion protein containing amino acids 32−579 of FAAH. WT-FAAH was also successfully expressed with an N-terminal His tag; however, subsequent attempts to purify this form of the enzyme proved to be exceedingly difficult, and therefore, the enzyme was expressed as a C-terminal His_6-tagged fusion protein. While a portion of the expressed enzymes was observed by Western blotting in insoluble inclusion bodies under all conditions, significant quantities of active protein could be recovered after a 4 h induction period with 1 mM IPTG. Induction for longer times resulted in a progressive loss of recoverable active FAAH, culminating at an induction time of 24 h where no active enzyme was isolated and all FAAH immunoreactivity was identifed in inclusion bodies. These results highlight the delicate nature of efficiently expressing eukaryotic membrane proteins in *E. coli* and indicate that carefully controlled induction protocols may facilitate the successful recombinant expression of other membrane proteins in this organism. Following cell lysis and solubilization with 1% Triton X-100, purification of the recombinant proteins was achieved using sequential Talon Metal Affinity Resin (Clontech) and heparin−agarose chromatography steps (Figure 3). Typical yields of purified WT- and ΔTM-FAAH ranged from 1 to 1.5 mg of protein per liter of culture volume.

Enzymology of Purified WT- and ΔTM-FAAH. To evaluate the effects of transmembrane domain deletion and/or recombinant expression on the enzymatic properties of FAAH, the purified recombinant proteins were compared to the native protein from rat liver. The two recombinant enzymes were found to exhibit pH−rate profiles nearly identical to that of the native enzyme, with maximal activity at pH 9.5 (Figure 4A). The only notable difference in the pH−rate profiles of the recombinant FAAHs was observed at pH 11.0, where the native enzyme was still significantly active while recombinant WT- and ΔTM-FAAH were completely inactive. On a similar note, we have observed that a 100 mM Na_2CO_3 incubation (30 min at 4 °C and pH 11.0) destroyed the catalytic activity of both WT- and ΔTM-FAAH derived from transfected COS-7 cells, whereas the native liver-isolated FAAH was stable to this treatment.

Lineweaver−Burk plots of the purified WT- and ΔTM-FAAH at pH 9.0 gave K_m values for oleamide of 23 ± 8 and 12 ± 2 μM, respectively (Figure 4B). These values were similar to the K_m value of 31 ± 3 μM found for native solubilized rat liver FAAH (*40*) and also compared well with previously reported K_m values for oleamide of 5 μM from nonsolubilized rat liver plasma membrane FAAH (*30*) and 9 and 14 μM from N18 mouse neuroblastoma-derived FAAH (*3*). On the basis of the estimated protein concentrations in the WT- and ΔTM-FAAH reactions, k_{cat} values of 7.1 and 3.3 s^{-1} were calculated for each enzyme, respectively, giving nearly identical k_{cat}/K_m values of 3.1×10^5 M^{-1} s^{-1} for WT-FAAH and 2.8×10^5 M^{-1} s^{-1} for ΔTM-FAAH. These k_{cat}/K_m values indicate that the efficiency of hydrolysis of oleamide by FAAH is comparable to that of most known protease- and amidase-catalyzed reactions.

Characterization of FAAH Self-Association. Upon purification from *E. coli*, the presence of SDS-resistant dimers of WT-FAAH, but not ΔTM-FAAH, was again observed by SDS−PAGE and Western blotting (Figure 5A). On 5 to 20% linear sucrose gradients, ΔTM-FAAH migrated near the 11.4 S standard (catalase), while WT-FAAH migrated as a very diffuse band beginning slightly larger than the 11 S catalase standard and extending beyond the 18 S thyroglobin standard (data not shown). Sucrose gradient-purified WT- and ΔTM-FAAH were subjected to sedimentation

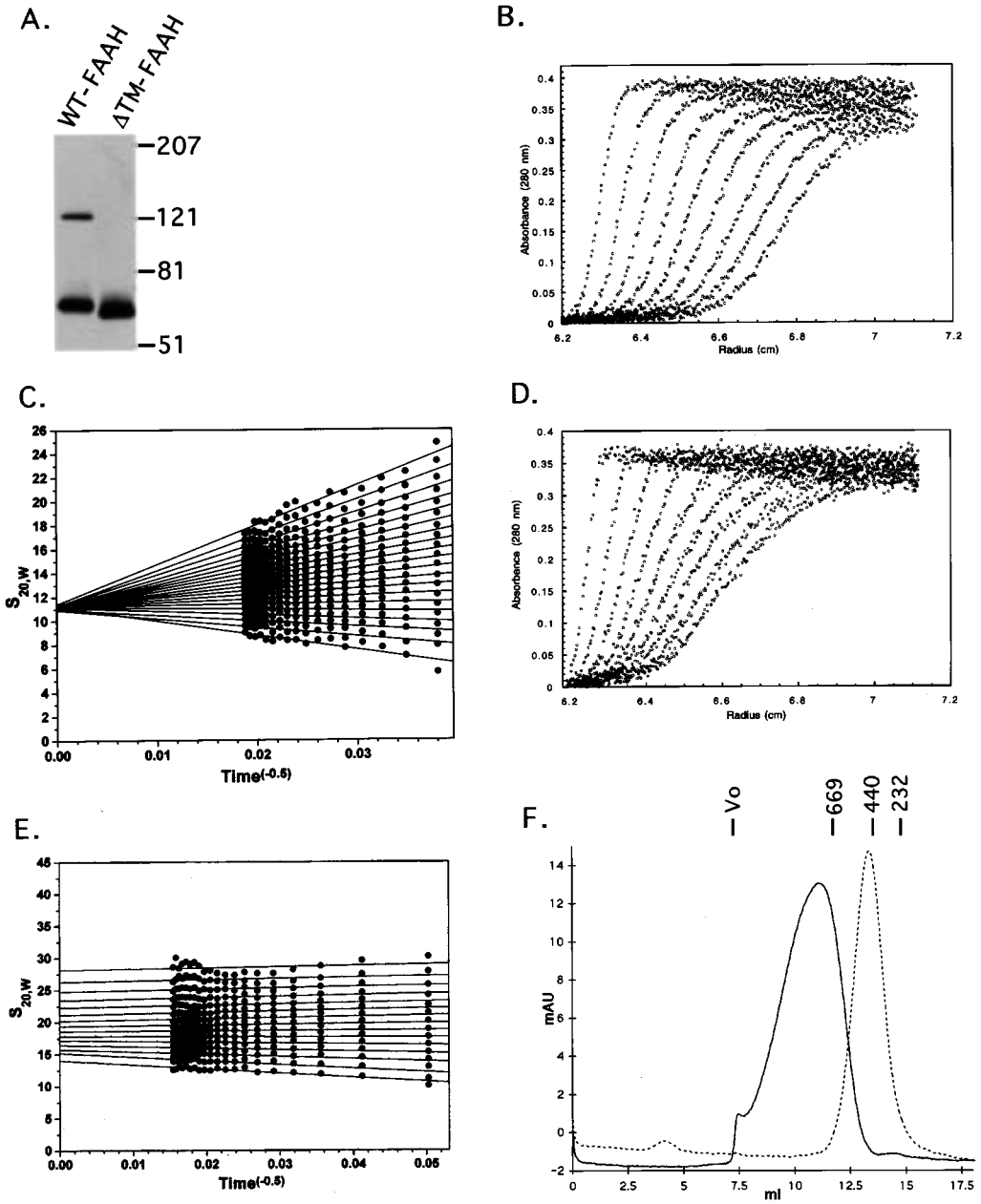

FIGURE 5: Characterization of the oligomeric states of recombinant WT- and ΔTM-FAAH. (A) WT-FAAH migrated as monomeric and dimeric species under reducing, denaturing conditions, while ΔTM-FAAH migrated as only a monomeric species. Molecular mass standards are indicated in kilodaltons. Sedimentation profiles (B and D; for clarity, scans shown are 7 min apart) and van Holde−Weischet extrapolation plots (C and E) of sedimentation velocity data collected at 40 000 rpm with 5 μM ΔTM-FAAH (B and C) and 30 000 rpm with 5 μM WT-FAAH (D and E). ΔTM-FAAH was a single 11 S species, while WT-FAAH behaved as a heterogeneous distribution of 15−28 S species. (F) Migration of ΔTM- (dashed line) and WT-FAAH (solid line) on Superose 6 gel filtration. Molecular mass standards are indicated in kilodaltons.

velocity and equilibrium ultracentrifugation analysis to characterize the self-association properties of these proteins (Figure 5B−E). Results from sedimentation velocity experiments indicated that detergent−protein complexes of ΔTM-FAAH existed primarily as a single species with an $s_{20,w}$ of 11.2 ± 0.2 S (Figure 5C). The 11.2 S species was found to be the dominant species over a concentration range of 1.25−10 μM. Attempts to determine the molecular mass of ΔTM-FAAH either by direct fitting of the absorbance profiles or from time derivative $g(*S)$ plots were complicated by small quantities (≤5%) of apparent aggregates which hindered the accurate evaluation of the diffusion coefficient. These analyses, however, typically yielded predicted molecular masses for ΔTM-FAAH between 165 and 260 kDa. Sedimentation equilibrium studies of ΔTM-FAAH were also complicated by an apparent self-association of the protein as it concentrated toward the bottom of the cell (data not shown); however, the smallest species observed in these studies, 260 kDa, was consistent with results obtained from sedimentation velocity analysis.

Detergent−protein complexes of WT-FAAH behaved as much larger 15−28 S species on the basis of sedimentation velocity analysis (Figure 5E). At all concentrations (from 2.5 to 10 μM) and under all conditions tested, the 15 S species was the smallest observed for WT-FAAH, even when the sample was analyzed in the presence of 0.4 M urea (data not shown). Time derivative analysis of the concentration profile indicated that the WT-FAAH sample consisted of

multiple species with two major sedimenting forms at 17 and 24 S that were partially resolved at later time points in the run. Due to the heterogeneity of species in the WT-FAAH sample, accurate determination of the molecular mass or oligomeric state of the protein could not be achieved.

In efforts to account for the possibility of bound detergent affecting the observed sedimentation velocity profiles of the two proteins, sedimentation velocity analysis of the FAAH proteins was performed in the presence of the neutrally buoyant detergent *n*-octyl pentaoxyethylene at 15 mM (C_8E_5, Bachem), in place of CHAPS (*41*). Both WT- and ΔTM-FAAH were observed to aggregate to a much larger extent in this detergent than in CHAPS, with 15−20% of each protein sample sedimenting quickly as high-molecular mass aggregates. However, time derivative analysis of the slower sedimenting boundary revealed essentially the same species for ΔTM-FAAH (12 S) and WT-FAAH (16−26 S) as those obtained in CHAPS.

Gel filtration chromatography of the purified FAAH samples also demonstrated that both WT- and ΔTM-FAAH behaved as large oligomeric species. WT-FAAH eluted in the void volume of a Superdex 200 column (Amersham Pharmacia Biotech), just before the 669 kDa thyroglobin standard, while ΔTM-FAAH eluted as a single peak slightly ahead of the 440 kDa ferritin standard with a predicted molecular mass of approximately 480 kDa (data not shown). A C-terminally His-tagged ΔTM-FAAH displayed an elution profile identical to that of the N-terminally His-tagged ΔTM-FAAH, indicating that the position of the histidine tag did not affect the migration properties of the protein. On a Superose 6 column, WT-FAAH eluted as a broad peak with a predicted molecular mass of approximately 850 kDa, while ΔTM-FAAH behaved as a 420 kDa species (Figure 5F). Analysis of the proteins loaded over a 100-fold initial concentration range (2−200 μM) yielded identical elution profiles (data not shown). Additionally, both proteins were analyzed in the presence of 2 mM lauryldimethylamine oxide (LDAO) in place of CHAPS as the buffer detergent and showed the same elution profiles under these conditions (data not shown).

Characterization of a FAAH Transmembrane Domain−GST Fusion Protein. To evaluate whether the presence of FAAH's N-terminal transmembrane domain region was sufficient to induce specific self-association, a GST fusion protein was constructed with FAAH's 39 N-terminal amino acid residues attached to the N terminus of GST (TM−GST). The fusion protein was expressed, purified by sequential glutathione−Sepharose and gel filtration chromatography steps, and analyzed by immunoblotting, gel filtration, and sedimentation velocity ultracentrifugation.

Results from SDS−PAGE Western blotting experiments revealed the presence of large amounts of SDS-resistant dimeric TM−GST, as well as faint larger bands potentially corresponding to trimeric and/or tetrameric species (Figure 6A). Purified GST was not found to form any SDS-resistant oligomers. The relative amounts of the TM−GST SDS-resistant oligomers were somewhat temperature dependent (data not shown), but even after boiling the protein for 10 min in SDS−PAGE loading buffer, a significant amount of SDS-resistant dimer was still observed. The TM−GST fusion protein could be fully separated from GST by gel filtration using a Superdex 200 column (Figure 6B). GST eluted slightly later than the 65 kDa marker (bovine serum albumin), as expected for its predicted dimeric size of 56 kDa, while TM−GST ran as an apparent heterogeneous population of species eluting partially in the void volume of the column and peaking slightly before the 440 kDa ferritin marker. Sedimentation velocity ultracentrifugation analysis of TM−GST supported the results from gel filtration indicating that the TM−GST sample contained a heterogeneous distribution of large oligomeric species (Figure 6C). The majority of the species observed were between 7 and 22 S, while trace amounts of larger oligomers were also apparent. In contrast, GST behaved as a single 3.5 S species with a predicted molecular mass of 46 kDa.

DISCUSSION

The amidase signature sequence enzymes represent a growing family of proteins found in a variety of both prokaryotic and eukaryotic organisms. Members of this enzyme family include indoleacetamidase from the plant pathogen *Agrobacterium tumefaciens* (*10*), which is involved in the production of the plant hormone indoleacetic acid (*42*), and acetamidase, a highly regulated enzyme from *Aspergillus nidulans* (*11*, *43*) that allows this organism to use acetamide as its sole carbon and nitrogen source (*44*, *45*). A single mammalian amidase signature sequence enzyme has been characterized to date, fatty acid amide hydrolase (FAAH), which is responsible for degrading bioactive fatty acid amides such as anandamide and oleamide (*1*). Despite the apparent importance of the amidase signature sequence family in a variety of signaling cascades, little is presently known about the catalytic and structural features of these enzymes. In this regard, a recent mutagenesis study conducted on the *Rhodoccocus rhodochrous* J1 amidase (*46*), indicates that this enzyme family does not hydrolyze amides by a classically defined protease mechanism and instead may operate by a novel mode of catalysis.

An apparently unique feature of FAAH when compared to other characterized members of the amidase signature family is the presence of a predicted N-terminal transmembrane domain (amino acids 9−29). To examine the role of this domain in FAAH structure and function, N-terminal transmembrane domain deletion constructs were produced that allowed for expression and analysis of this mutant protein (ΔTM-FAAH) in both COS-7 cells and *E. coli*. Expression of ΔTM-FAAH in COS-7 cells demonstrated that deletion of FAAH's predicted N-terminal transmembrane domain did not abolish FAAH's ability to interact strongly with membranes. It is perhaps not unexpected that extensive membrane interactions beyond those provided by a single membrane-spanning domain would be exhibited by FAAH. Such strong membrane associations in the absence of transmembrane domains have previously been observed for other enzymes such as prostaglandin H synthase (*47*) and squalene cyclase (*48*), which bind the membrane through hydrophobic patches that penetrate one leaflet of the bilayer. These membrane interactions are thought to be central to efficient enzymatic catalysis, facilitating both substrate binding and product release (*48*). A FAAH−membrane association similar in type to the membrane contacts displayed by prostaglandin H synthase and squalene cyclase could allow bilayer-embedded fatty acid amides direct access to FAAH's catalytic machinery.

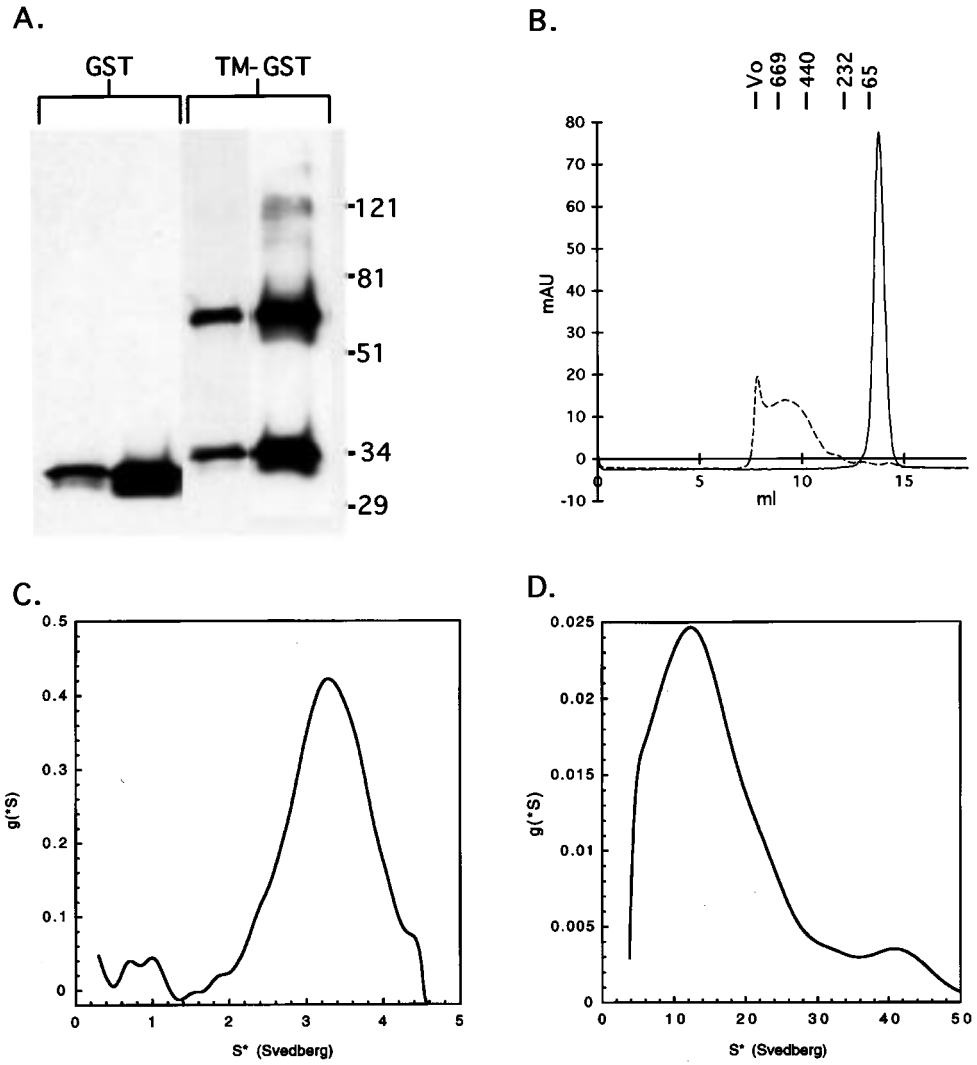

FIGURE 6: Characterization of assembly of a FAAH transmembrane domain−GST fusion protein (TM−GST). (A) SDS-resistant oligomeric species of TM−GST (right lanes) but not control GST (left lanes) were observed by Western blotting. A low and high exposure of each protein sample is shown. Proteins were run on a 4 to 20% polyacrylamide gradient gel. Molecular mass standards are indicated in kilodaltons. (B) Gel filtration analysis of GST (solid line) and TM−GST (dashed line) indicating the presence of large oligomeric species for TM−GST. (C and D) Time derivative $g(*S)$ analysis of the concentration profile of GST (C) and TM−GST (D) from sedimentation velocity data. Note the different scales for the *x*-axis ($S*$) of panels C and D.

Having deduced that FAAH does not require its N-terminal transmembrane domain to interact strongly with membranes, we arrived at the following question: what function might this region of the enzyme serve? Initial enzymatic studies of WT- and ΔTM-FAAH from transfected COS-7 cells demonstrated that both enzymes were catalytically active in crude homogenates. Moreover, oleamide added to both WT- and ΔTM-FAAH-transfected COS-7 cells in culture was more rapidly degraded than oleamide added to mock-transfected COS-7 cells, indicating that ΔTM-FAAH was able to access its substrates in vivo. Finally, the enzymatic properties of purified recombinant WT- and ΔTM-FAAH were nearly identical, indicating that the N-terminal transmembrane domain of FAAH does not play a direct role in the catalytic activity of the enzyme.

One notable difference observed between WT- and ΔTM-FAAH, both in COS-7 and in *E. coli* expression systems, was the ability of WT-FAAH, but not ΔTM-FAAH, to form SDS-resistant oligomers. Cross-linking of the two enzymes on COS-7 cell membranes with the sulfhydryl reactive cross-linker BMH revealed that both enzymes appeared to be oligomeric when membrane-bound. Additionally, cross-linking of WT-FAAH consistently generated a larger proportion of a tetrameric species than cross-linking of ΔTM-FAAH, perhaps indicating differences in the oligomerization properties for each enzyme. However, given that the transmembrane domain of FAAH possesses two potentially cross-linkable cysteines, the differences in the cross-linking profiles observed for the two enzymes do not necessarily reflect differences in their respective oligomerization states.

Sedimentation velocity analytical ultracentrifugation and gel filtration analysis of the purified recombinant enzymes confirmed the ability of FAAH to form homo-oligomeric complexes, and indicated differences in the relative oligomeric states of WT- and ΔTM-FAAH. In buffer solutions containing 0.5% CHAPS, ΔTM-FAAH sedimented as a single oligomeric species with an *s* value of 11.2 S, and eluted on gel filtration columns slightly before the 440 kDa marker while WT-FAAH sedimented as a heterogeneous distribution of species with *s* values ranging from 15 to 28 S and eluted as a broad peak ahead of the 669 kDa marker. The absence of any observed protein concentration effects

for the oligomeric sizes of WT- and ΔTM-FAAH suggests that the FAAH is likely to be an oligomeric protein at the lower enzyme concentrations used in enzyme assays and found in vivo.

The molecular mass of ΔTM-FAAH determined directly from the sedimentation velocity data varied from 165 to 260 kDa depending on the method employed (direct fitting or time derivative analysis). These values were significantly smaller than the molecular masses estimated by gel filtration (420 kDa on Superose 6 and 480 kDa on Superdex 200). Using the Stokes radius obtained from gel filtration (relative to the standards of known Stokes radii) to calculate a diffusion coefficient, and the $s_{20,w}$ value determined by sedimentation velocity analysis, a molecular mass of 300−350 kDa was calculated for the detergent−enzyme complex. Sedimentation studies in the neutrally buoyant detergent C_8E_5 and gel filtration in LDAO yielded *s* values and elution profiles nearly identical to those found in CHAPS, indicating that the contribution of bound detergent to the measured hydrodynamic parameters was likely relatively small. Thus, depending on the exact method employed for analysis of the data, the predicted oligomeric state of the enzyme ranged from trimeric to heptameric. On the basis of the apparent discrepancies between the these methods, defining the precise oligomeric state of ΔTM-FAAH will require further study. These data, however, do support a trimeric or larger oligomeric state for this enzyme.

Both sedimentation velocity analysis and gel filtration studies suggested that WT-FAAH, when expressed in *E. coli*, was a heterogeneous distribution of oligomeric species, all of which were apparently larger than the species found for ΔTM-FAAH. It is presently not clear whether the heterogeneity of this sample is relevant to the state of the enzyme in vivo. The interactions giving rise to the heterogeneous population are certainly specific, as the species observed were consistent in several independent preparations and under several conditions. The oligomerization of ΔTM-FAAH, in the absence of the transmembrane domain, suggests that multiple oligomerization sites exist in FAAH. It is possible that the prokaryotic translational machinery is unable to properly assemble the transmembrane domain containing enzyme into its native oligomeric state due to the complexity of interactions found for the protein. This possibility is supported by the observation that the relative amount of SDS-resistant dimer observed for the *E. coli*-expressed WT-FAAH was consistently higher than that found in COS-7 cells, while SDS-resistant oligomeric forms larger than dimer were rarely observed with the *E. coli*-derived WT-FAAH. Further studies will be required to determine whether self-association through FAAH's transmembrane domain causes FAAH to form higher-order oligomers in vivo, or instead serves to stabilize the oligomeric state observed in its absence.

The ability of FAAH's transmembrane domain region to self-associate was further studied by fusing the 39 N-terminal amino acids of FAAH to the N terminus of GST. As expected for a homo-oligomeric interaction, the TM−GST construct was able to form SDS-resistant dimers and larger forms similar to WT-FAAH. These species were present even in crude bacterial lysates, indicating that the self-association was specific (data not shown). Since GST is a dimer with its N termini facing in opposite directions (*49*), we anticipated that self-association through FAAH's transmembrane domain might result in polymerization of TM−GST into very large oligomers (*50*). This was found to be the case for TM−GST based on size exclusion chromatography and sedimentation velocity analysis. While this polymerization of TM−GST provided an easily detectable change in oligomeric state, this fusion protein did not allow for a means of assessing whether FAAH's transmembrane domain could oligomerize to states higher than dimers. Further structural and biochemical studies with monomeric fusion proteins containing the FAAH transmembrane domain may assist in elucidating the stoichiometry of this association.

It is clear from these studies that FAAH's transmembrane domain region can function as an autonomous oligomerization site. The ability of transmembrane domains to form specific, and often SDS-resistant, homo-oligomeric structures has been demonstrated for a small but growing family of proteins (*51*). The most well studied example of a protein that forms transmembrane domain-mediated homodimers is glycophorin A, whose transmembrane domain, like that of FAAH, is sufficient to induce dimerization in the context of a heterologous fusion protein (*52*). Interestingly, recent structural information on a dimer of the glycophorin A transmembrane domain has shown that van der Waals interactions alone suffice to generate stable and specific molecular self-association (*53*).

Specific transmembrane domain interactions of single membrane helix proteins have generally been observed in receptor proteins. Thus, it is intriguing that an enzyme like FAAH would display this means of self-association, especially given that deletion of FAAH's transmembrane domain does not appear to affect enzymatic activity. It is possible that the presence of FAAH's transmembrane domain is necessary for the localization and/or stability of the enzyme in its native environment. An alternative, and perhaps more provocative hypothesis, however, is that this added level of structural complexity could be indicative of additional roles for FAAH in cell signaling processes.

ACKNOWLEDGMENT

We thank P. Schimmel, N. B. Gilula, M. H. Bracey, and J. S. Rosenblum for helpful discussions and critical readings of the manuscript and all members of the Cravatt and Kelly labs for advice and assistance.

REFERENCES

1. Cravatt, B. F., Giang, D. K., Mayfield, S. P., Boger, D. L., Lerner, R. A., and Gilula, N. B. (1996) *Nature 384*, 83.
2. Chin, S., and Deutsch, D. G. (1993) *Biochem. Pharmacol. 46*, 791.
3. Maurelli, S., Bisogno, T., De Petrocellis, L., Di Luccia, A., Marino, G., and Di Marzo, V. (1995) *FEBS Lett. 377*, 82.
4. Desarnaud, F., Cadas, H., and Piomelli, D. (1995) *J. Biol. Chem. 270*, 6030.
5. Ueda, N., Kurahashi, Y., Yamamoto, S., and Tokunaga, T. (1995) *J. Biol. Chem. 270*, 23823.
6. Mayaux, J.-F., Cerbelaud, E., Soubrier, F., Faucher, D., and Petre, D. (1990) *J. Bacteriol. 172*, 6764.
7. Hashimoto, Y., Nishiyama, M., Ikehata O., Horinouchi, S., and Beppu, T. (1991) *Biochim. Biophys. Acta 1088*, 225.
8. Kobayashi, M., Komeda, H., Nagasawa, T., Nishiyama, M., Horinouchi, S., Beppu, T., Yamada, H., and Shimizu, S. (1993) *Eur. J. Biochem. 217*, 327.
9. Tsuchiya, K., Fukuyama, S., Kanzaki, N., Kanagawa, K., Negoro, S., and Okada, H. (1989) *J. Bacteriol. 171*, 3187.

10. Klee, H., Montoya, A., Horodyski, F., Lichtenstein, C., Garfinkel, D., Fuller, S., Flores, C., Peschon, J., Nester, E., and Gordon, M. (1984) *Proc. Natl. Acad. Sci. U.S.A. 81*, 1728.
11. Corrick, C. M., Twomey, A. P., and Hynes, M. J. (1987) *Gene 53*, 63.
12. Giang, D. K., and Cravatt, B. F. (1997) *Proc. Natl. Acad. Sci. U.S.A. 94*, 2238.
13. Ettinger, R. A., and DeLuca, H. F. (1995) *Arch. Biochem. Biophys. 316*, 14.
14. Cravatt, B. F., Prospero-Garcia, O., Siuzdak, G., Gilula, N. B., Henriksen, S. J., Boger, D. L., and Lerner, R. A. (1995) *Science 268*, 1506.
15. Devane, W. A., Hanus, L., Breuer, A., Pertwee, R. G., Stevenson, L. A., Griffin, G., Gibson, D., Mandelbaum, A., Etinger, A., and Mechoulam, R. (1992) *Science 258*, 1946.
16. Facci, L., Dal toso, R., Romanello, S., Buriani, A., Skaper, S. D., and Leon, A. (1995) *Proc. Natl. Acad. Sci. U.S.A. 92*, 3376.
17. Wakamatsu, K., Masaki, T., Itoh, F., Koichi, K., and Sudo, K. (1990) *Biochem. Biophys. Res. Commun. 168*, 423.
18. Barg, J., Fride, E., Hanus, L., Levy, R., Matus-Leibovitch, N., Heldman, E., Bayewitch, M., Mechoulam, R., and Vogel, Z. (1995) *Eur. J. Pharmacol. 287*, 145.
19. Smith, P. B., Compton, D. R., Welch, S. P., Razdan, R. K., Mechoulam, R., and Martin, B. R. (1994) *J. Pharmacol. Exp. Ther. 270*, 219.
20. Lerner, R. A., Siuzdak, G., Prospero-Garcia, O., Henriksen, S. J., Boger, D. L., and Cravatt, B. F. (1994) *Proc. Natl. Acad. Sci. U.S.A. 91*, 9505.
21. Hiudobro-Toro, J., and Harris, R. A. (1996) *Proc. Natl. Acad. Sci. U.S.A. 93*, 8078.
22. Thomas, E. A., Carson, M. J., Neal, M. J., and Sutcliffe, J. G. (1997) *Proc. Natl. Acad. Sci. U.S.A. 94*, 14115.
23. Boger, D. L., Patterson, J. E., and Jin, Q. (1998) *Proc. Natl. Acad. Sci. U.S.A. 95*, 4102.
24. Thomas, E. A., Cravatt, B. F., Danielson, P. E., Gilula, N. B., and Sutcliffe, J. G. (1997) *J. Neurosci. Res. 50*, 1047.
25. Egertova, M., Giang, D. K., Cravatt, B. F., and Elphick, M. R. (1998) *Proc. R. Soc. London, Ser. B* (in press).
26. Koutek, B., Prestwich, D. G., Howlett, A. C., Chin, S. A., Salehani, D., Nima, A., and Deutsch, D. G. (1994) *J. Biol. Chem. 269*, 22937.
27. Bisogno, T., Sepe, N., De Petrocellis, L., Mechoulam, R., and Di Marzo, V. (1997) *Biochem. Biophys. Res. Commun. 239*, 473.
28. Romero, J., Garcia-Palomero, E., Lin, S. Y., Ramos, J. A., Makriyannis, A., and Fernandez-Ruiz, J. J. (1996) *Life Sci. 58*, 1249.
29. Le Maire, M., Aggerbeck, L. P., Monteilhet, C., Andersen, J. P., and Møller, J. V. (1986) *Anal. Biochem. 154*, 525.
30. Patterson, J. E., Ollman, I. R., Cravatt, B. F., Boger, D. L., Wong, C. H., and Lerner, R. A. (1996) *J. Am. Chem. Soc. 118*, 5938.
31. Van Holde, K. E., and Weischet, W. O. (1978) *Biopolymers 17*, 1387.
32. Hansen, J. C., Lebowitz, J., and Demeler, B. (1994) *Biochemistry 33*, 13155.
33. Demeler, B., Saber, H., and Hansen, J. C. (1997) *Biophys. J. 72*, 397.
34. Stafford, W. F., III (1992) *Anal. Biochem. 203*, 295.
35. Stafford, W. F., III (1994) *Methods Enzymol. 240*, 478.
36. Laue, T. (1992) in *Analytical Ultracentrifugation in Biochemistry and Polymer Science*, pp 63−89, Redwood Press Ltd., Cambridge, England.
37. Durchschlag, H. (1986) in *Thermodynamics Data for Biochemistry and Biotechnology* (Hinz, H.-J., Ed.) pp 45−127, Springer-Verlag, New York.
38. McMeekin, T. L., and Marshall, K. (1952) *Science 116*, 142.
39. Perkins, S. J. (1986) *Eur. J. Biochem. 157*, 169.
40. Patricelli, M. P., Patterson, J. E., Boger, D. L., and Cravatt, B. F. (1998) *Bioorg. Med. Chem. Lett. 8*, 613.
41. Fleming, K. G., Ackerman, A. L., and Engelman, D. M. (1997) *J. Mol. Biol. 272*, 266.
42. Thomashow, M. F., Hugly, S., Buchholz, W. G., and Thomashow, L. S. (1986) *Science 231*, 616.
43. Davis, M. A., Kelly, J. M., and Hynes, M. J. (1993) *Genetics 90*, 133.
44. Hynes, M. J. (1975) *Aust. J. Biol. Sci. 28*, 301.
45. Hynes, M. J., and Kelly, J. M. (1977) *Mol. Gen. Genet. 150*, 193.
46. Kobayashi, M., Fujiwara, Y., Goda, M., Komeda, H., and Shimizu, S. (1997) *Proc. Natl. Acad. Sci. U.S.A. 94*, 11986.
47. Picot, D., Loll, P. J., and Garavito, R. M. (1994) *Nature 367*, 243.
48. Wendt, K. U., Poralla, K., and Shulz, G. E. (1997) *Science 277*, 1811.
49. McTigue, M. A., Williams, D. R., and Tainer, J. A. (1995) *J. Mol. Biol. 246*, 21.
50. Riley, L. G., Ralston, G. B., and Weiss, A. S. (1996) *Protein Eng. 9*, 223.
51. Borman, B. J., and Engelman, D. M. (1992) *Annu. Rev. Biophys. Biomol. Struct. 21*, 223.
52. Lemmon, M. A., Flanagan, J. M., Treutlein, H. R., Zhang, J., and Engelman, D. M. (1992) *Biochemistry 31*, 12719.
53. MacKenzie, K. R., Prestegard, J. H., and Engelman, D. M. (1997) *Science 276*, 131.

BI981733N